Available online at www.sciencedirect.com
ScienceDirect
Journal of Sound and Vibration 305 (2007) 659–671
JOURNAL OF SOUND AND VIBRATION
www.elsevier.com/locate/jsvi

Visualising scattering underwater acoustic fields using laser Doppler vibrometry

A.R. Harland, J.N. Petzing*, J.R. Tyrer

Wolfson School of Mechanical and Manufacturing Engineering, Loughborough University, Loughborough, Leicestershire, LE11 3TU, UK

Received 11 April 2006; received in revised form 4 April 2007; accepted 17 April 2007
Available online 22 June 2007

Abstract

Analysis of acoustic wavefronts are important for a number of engineering design, communication and health-related reasons, and it is very desirable to be able to understand the interaction of acoustic fields and energy with obstructions. Experimental analysis of acoustic wavefronts in water has traditionally been completed with single or arrays of piezoelectric or magnetostrictive transducers or hydrophones. These have been very successful, but the presence of transducers within the acoustic region can in some circumstances be undesirable. The research reported here, describes the novel application of scanning laser Doppler vibrometry to the analysis of underwater acoustic wavefronts, impinging on circular cross section obstructions. The results demonstrate that this new non-invasive acoustics measurement technique can successfully visualise and measure reflected acoustic fields, diffraction and refraction effects.

1. Introduction

The understanding of acoustics has developed over many decades, both in terms of the theoretical development, as well as the experimental analysis. This has led to many applications of acoustics, ranging from sensitive listening devices to destructive medical devices.

The transmission of sound through water has been the topic of significant study, providing descriptions of the variation of acoustic velocity in water with respect to factors such as temperature, pressure and salinity [1–4]. Experimental analysis of water-based and underwater acoustics relies upon the use of traditional piezoelectric-based transducers, commonly known as hydrophones. These are typically point source/receiver devices which provide excellent two-dimensional temporal resolution but poor spatial resolution. In order to generate three-dimensional maps of acoustic pressure, and to ''visualise'' acoustic wavefronts, it is necessary to scan a single hydrophone through the acoustic volume, or construct arrays of hydrophones (whose resolution is a function of the number of transducers in the array and their spacing) An example of a hydrophone array used for calibration purposes is described by Preston [5]. The dimensions of the hydrophones used are typically specified with respect to the wavelength of the acoustic signals being analyzed.

*Corresponding author. Tel.: +44 1509 227617; fax: +44 1509 227648.
E-mail address: j.petzing@lboro.ac.uk (J.N. Petzing).

0022-460X/$ - see front matter © 2007 Elsevier Ltd. All rights reserved.
doi:10.1016/j.jsv.2007.04.026

Despite their prevalence, data from transducer arrays cannot be considered ideal due to the potential perturbation caused by the physical presence of the transducers and their supporting structure.

The desire to understand acoustic wavefronts and their interaction with objects has motivated acousticians for many years. To be able to routinely visualise acoustic interactions would enhance the acoustic designer's ability to optimise both the performance of acoustic sources and detectors, and allow the generation of structures, surfaces and materials with particular acoustic absorption and scattering characteristics. It has therefore been desirable to consider alternative solutions to the task of acoustic field measurement and visualisation, with specific emphasis towards two-dimensional analyses leading on to the potential of tomographic analysis.

The most promising approach to developing new transducers capable of visualising acoustic wavefronts has been to consider optical metrology techniques. Single point optical transducers are already used in calibration laboratories, with the UK primary standard for underwater acoustic calibrations in the frequency range 500 kHz to 15 MHz, being based on a Michelson interferometer first suggested by Drain et al. [6], refined by Bacon et al. [7] in 1986 and adopted by the National Physical Laboratory (NPL) in 1987. While this technique is largely non-perturbing (it does not require the presence of any bodies of significant dimensions to be submerged in the field), a 3- or 5-μm-thick optically reflective PVDF pellicle is required to return the laser light, although it is assumed that this membrane does not influence acoustic propagation [8]. Given this successful application of optical metrology, much attention has been given to the development of future measurement techniques based on optical methods.

One important consideration when applying optical metrology solutions to acoustic analysis, is the interaction of light energy and acoustic energy, with the key parameter being the refractive index of the media. Initial work in this area can be traced to the first half of the twentieth century [9,10], although it was the work of Raman and Nath [11,12], which established a sound theoretical basis. The topic of ultrasonically induced diffraction has been the subject of many reviews, with one of the more recent considering high-frequency acoustic measurements by optical techniques [13].

Specific examples of previously reported applications of optical metrology techniques can be identified as Schlieren [14], Michelson interferometry [15], electronic speckle pattern interferometry (ESPI) [16,17] and laser Doppler anemometry (LDA) [18]. The use of Michelson interferometry and LDA for acoustic analyses are both limited by the fact that they are single point techniques with no volumetric capability. Conversely, Schlieren and ESPI are inherently wholefield in their analytical approach, but Schlieren is very much a qualitative technique and ESPI has demonstrated poor signal-to-noise ratios.

An alternative technique which has more recently been demonstrated is that of laser Doppler vibrometry (LDV). Application of LDV to acoustic measurements in air have been documented [17,19–21], although chronologically, these reports have occurred at the same time as water-based experimentation. One of the earliest applications of LDV in underwater acoustics was the successful monitoring of the passage of a surface wave during its propagation over an aluminium plate [22]. In a hybrid system based on the principle of operation of the NPL laser interferometer [7], a method for deriving underwater acoustic particle velocity through measurements from a suspended pellicle was reported [23]. The technique was found to benefit over the NPL laser interferometer from increased simplicity and its ability to resolve acoustic signals from extraneous low-frequency vibrations.

The extent of LDV application has, however, been limited to using a secondary target within the acoustic medium, which reduces the non-contact non-perturbing potential of the transducer. Recent work has considered the interaction of the laser beam itself, with the acoustic energy, thus providing a direct measure of acoustic energy [24,25] utilising the refractive index of the media varying with changes in acoustic pressure. This work compares well with other research [26], demonstrating that a LDV transducer can be passed through the acoustic field generated by a piezoelectric transducer and produce temporal signals that correlate well with traditional hydrophone measurements. Furthermore, by scanning the laser through the acoustic field, it has been demonstrated that two-dimensional images of acoustic waves and fields can be mapped and identified [27,28]. Aspects of this work have been taken further by other researchers with analysis of external error contributions [29], comparison with radiation force balances [30], further analysis of LDV as a new primary standard for underwater acoustics [31] and comparison with wholefield optical metrology techniques [32].

The purpose of this paper is to report initial quantitative results from the novel application of scanning LDV to the study of acoustic energy reflected and diffracted by objects placed within an underwater acoustic field. Objects of different sizes and structure with respect to the wavelength of the acoustic source have been used to illustrate a range of acoustic phenomena, specifically being visualised and measured in real-time by the LDV technique.

2. Laser Doppler vibrometry

LDV, sometimes known as velocimetry, is a well-established tool used primarily to record velocity measurements from the scattering elements of solid surface targets [33]. The principle of operation and the equipment used in LDV experimentation is intrinsically the same as that of LDA, the major difference being the use of the two beams between which the frequency difference is observed. In LDV (shown in Fig. 1), the two beams created from the laser source by beam splitter (BS1) are diverted such that only one is used to illuminate the target. The other 'reference' beam follows a path through a homogeneous medium usually sufficiently long enough to compensate for any coherence length discrepancy before being recombined with the target beam (at BS3). Standard commercially available LDV equipment, detects the frequency shift in back scattered light from the target. The geometry used is based on that of the Michelson interferometer and is typical of that originally proposed in literature [34].

Since the frequency of the returning light is too high to be measured directly by any opto-electric detector, it is mixed with the reference beam to create a measurable heterodyne frequency (BS3). Signals generated in this way are directionally ambiguous due to the heterodyne frequency representing the difference in frequency between the two beams. For this reason, a frequency shift produced by a Bragg cell, diffraction grating or rotating target is included in one of the arms (via BS2) to offset the resultant heterodyne or beat frequency from zero. The photodetectors (D_1 and D_2) provide an output proportional to the intensity of the incident light. This is then demodulated to provide a voltage output proportional to the velocity of the target.

Initial analysis of LDV in the context of underwater acoustic analysis, considers the ideal case of a collimated acoustic beam of radius r, with plane phase fronts. Considering the simplest geometry of a single point LDV transducer, the beam from the LDV is normal to the axis of the acoustic field. In this arrangement, the acoustic phase, Φ, remains constant with distance along the line and the voltage output from the LDV, V, which is proportional to the rate of change of optical path length, is described by Eq. (1), where K is the sensitivity scalar of the LDV electronics, $(\partial n/\partial P)_S$ the adiabatic piezo-optic coefficient, A the acoustic pressure

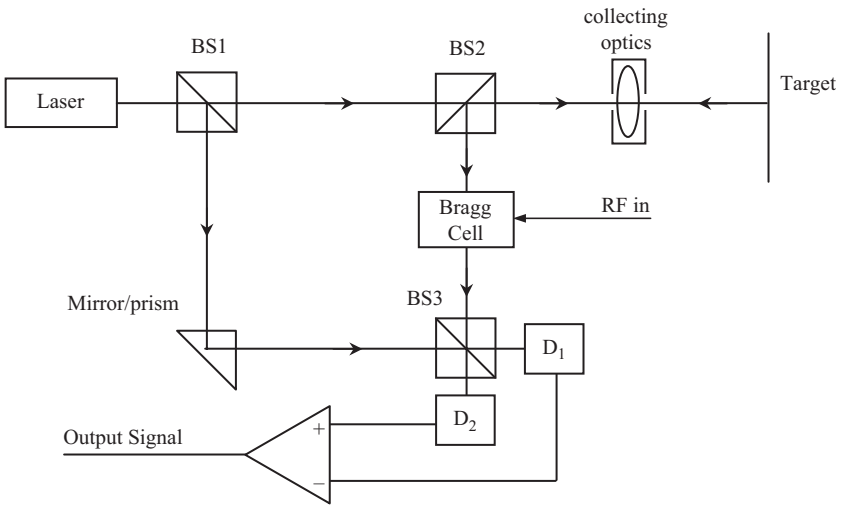

Fig. 1. Basic schematic of a laser Doppler vibrometer.

amplitude and f the acoustic frequency [27]:

$$V(t) = K\frac{\mathrm{d}l(t)}{\mathrm{d}t} = 8\pi rK\left(\frac{\partial n}{\partial P}\right)_S A\cos(2\pi ft - \Phi). \tag{1}$$

The optical path length, l, represents the integral of the refractive index, n, with distance, where the limits of integration are of the path of the laser beam that is affected by the sound field. Consequently, the laser transducer is able to map refractive index changes as a function of pressure variations, which act as the unique signature of each acoustic field.

In this particular study, a scanning laser vibrometer was used (Polytec OFV-056 Scan head and OFV-3001-S controller, frequency cut-off −1.5 MHz) to provide complete two-dimensional mapping of the acoustic volume. The details of the optical interrogation of the acoustic volume can be seen in Fig. 2, which identifies the issues of the angular movement of the laser beam. The scanning system allows the laser beam to be sequentially directed within a range specified by a number of discrete positions established on a fixed, stationary target beyond and outside the acoustic volume. With respect to a phase-locked reference trigger signal from the acoustic source, the scanning transducer is able to provide a referenced measurement of spatial and temporal pressure distribution (as a function of refractive index change).

The development of the acousto-optic theory has had to take into account several factors which complicate the analysis of a scanning transducer compared to the single line analysis of the simplified case shown in Eq. (1). For the purposes of the mathematical explanation, it is assumed that the field generated by the plane-piston acoustic source is perfectly collimated, although it is recognised that in reality this is highly unlikely. Consequently, the analysis needs to take into account when the laser beam is incident with arbitrary angles (polar angle ϕ and elevation angle θ as shown in Fig. 2) on the acoustic beam. The optical path length, l, in this case can be written as

$$l = l_0 + A_0\left(\frac{\partial n}{\partial p}\right)\int_{S_1}^{S_2}\sin[\omega t - k(x_0 + |S|\cos\,\theta\,\sin\phi)]\,\mathrm{d}s, \tag{2}$$

where $k = \omega/c$ is the acoustic wavenumber and l_0 the ambient optical path length. If the line integral is then calculated, Eq. (2) can be rewritten as

$$l(t) = l_0 + A_0\left(\frac{\partial n}{\partial p}\right)\frac{1}{\alpha}[\cos(\alpha|S_2| - \Psi) - \cos(\alpha|S_1| - \Psi)], \tag{3}$$

where $\alpha = k\cos\theta\sin\phi$ is the wavenumber projected onto the normal axis, $\Psi = \omega t - kx_0$ is the phase term when the beam is normal to the axis of the sound field, and the distances $|s_1|$ and $|s_2|$ are indicated in Fig. 2.

Taking into account the Cartesian expansion of the terms $|s_1|$ and $|s_2|$ [27], the rate of change of optical path length (and consequently acoustic pressure) as measured by the scanning laser Doppler vibrometer can be

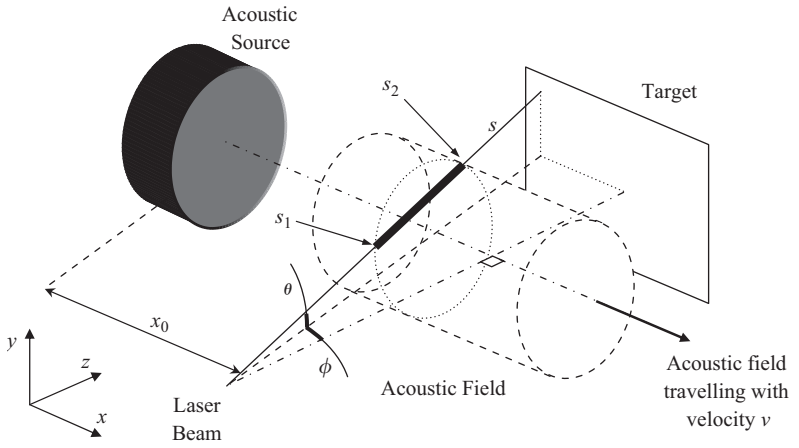

Fig. 2. Laser beam scanning through an acoustic volume.

summarised as

$$\frac{\mathrm{d}l(t)}{\mathrm{d}t} = 2A_0\left(\frac{\partial n}{\partial p}\right)\frac{\omega}{\alpha}[\sin(\omega t - (kx_0 - |s_1|\alpha)) - \sin(\omega t - (kx_0 - |s_2|\alpha))]. \quad (4)$$

It should be noted that the generation of this unique theoretical description for the application of LDV to acoustic field analysis must take into account certain limits, specifically that angular errors and approximations can be improved by ensuring that the transducer-acoustic field stand-off distance is significantly large, thus reducing the angular sweep of the volume, improving the approximation to normal transmission through the media.

In reality, while the acoustic source may approximate to plane wave output, reflection and refraction of the acoustic energy from the obstacles in the water will lead to complex wavefronts. As identified previously [19,20,27,28], all variations of refractive index along the measuring path have an influence on the measured result, and consequently, the rate of change of optical path length will be a mean value, except for the specialised case of normal transmission of the laser through a collimated acoustic plane wave.

Therefore in this context, it would be inappropriate for the quantified output of the scanning LDV to be represented in pressure terms, because this would produce a misleading map of pressure distribution, with areas which would be correct and areas which would be prone to increasing error content, especially at the extremities of the scan. Consequently, the quantified output of the experimentation has been given as the rate of change of optical path length.

Issues of instrument confidence have also been considered with this work. While primary and secondary procedures for accelerometers (and other devices) are covered under BS ISO 16063 [35], there is currently no formalised procedure for direct calibration of laser vibrometers. However, calibration can and is achieved via comparison standards with calibrated accelerometers and traceable mechanical shakers, although the extended frequency range capability of laser vibrometers often exceeds that of the accelerometers. Comparison calibrations of this nature are completed for Polytec vibrometers at the German National Laboratory (Physikalisch-Technische Bundesanstalt—PTB). The issue of calibrating across the extended frequency range is dealt with by injection of high-quality synthetic Doppler signals (traceable to the frequency/time standards) into the Doppler signal processing electronics, with accurate measurement of output analogue voltages [36].

This provides a definitive statement of instrument performance, which is defined as a sequence of calibrated scale factors. However, analysis of error budgets associated with the experimentation is very significantly more complex, because it has to contend with the interaction of the transducer with the experimental apparatus. Because of the issues discussed above, any error term will predominantly be a function of nonlinear integrating effects across the diverging acoustic volume, plus angle of volume interrogation. These two components have previously been assessed for the more specialist case of a non-scanning analysis of plane wave water-based acoustic propagation [29], clearly identifying the angular dependency of error terms, and the need to minimise their impact. In the study being reported here, these errors are unavoidable, and vary nonlinearly across the measurement volume.

At this point in time, this complex error budget has not been calculated. However, traceability of the experimentation and definition of minimum resolvable limits has been achieved via direct comparison with the UK NPL underwater pressure standard (NPL laser interferometer). These terms were assessed [25] as being $-82.4\,\mathrm{dB}/\sqrt{\mathrm{Hz}}$ re: 1 Pa for the noise floor, and $18.9\times10^{-3}\,\mathrm{Pa}/\sqrt{\mathrm{Hz}}$ minimum instrument sensitivity, although clearly these terms do not identify explicit statements of error budget.

3. Experimentation and results

Fig. 3 shows the experimental arrangement of the scanning LDV transducer and acoustic source. The LDV scanning head was positioned approximately 1 m from the acoustic axis. The laser beam traversed the width of the glass tank through the measurement volume (internal dimensions 1219 mm × 457 mm × 295 mm), was reflected by a stationary target consisting of a rigid panel of commercially available 3M retro-reflective material (100 mm × 100 mm) and returned along the same path to the vibrometer head. A measurement grid of specified increments in x and y was then established on the target, the nodes of which defined the measurement positions for the laser beam. It should be noted that there are merits in designing the acoustic system to be that

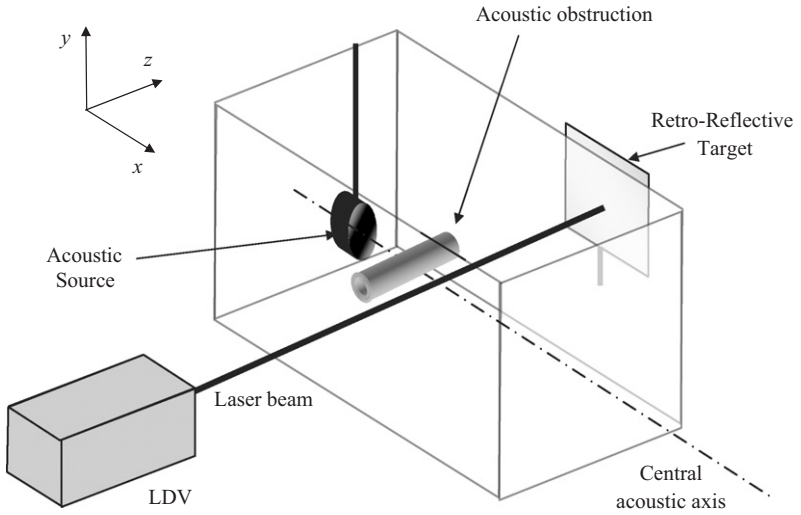

Fig. 3. Experimental set-up for acoustic obstruction analysis.

of a single mode wave-guide, but due to the complexity of reflected and refracted wavefronts, and consequently the averaging of the pressure distribution along any one laser path, this was deemed as being unnecessary and complements the reasoning of other researchers [19].

A time-resolved measurement of the rate of change of optical path length was recorded at each target position, triggered and phase locked in time from the acoustic source input signal. The distance of the measurement position from the source, the acoustic frequency and the number of acoustic cycles determined the measurement duration. The signal was sampled at 40 MHz and a fast Fourier transform (FFT) with a maximum resolution of 6400 lines was recorded in software. The original rate of change of path length data recorded by the vibrometer were extracted from the proprietary Polytec software in complex FFT form and converted into the time domain using *Matlab* [37], to enable measurements of the acoustic field within the water to be derived. The previously recorded angular positions were used to position each measurement point within the final image. A linear interpolation was undertaken between adjacent measurements to increase the number of pixels in each axis by a factor of 5, thus improving the visual quality of the images.

The magnitude or power at a certain frequency within a signal measured using an LDV was established from the respective FFT component of the magnitude or power spectrum at the excitation frequency. Each complex FFT was converted into a power spectrum and the component at the fundamental acoustic frequency was taken to represent the 'power' of the signal, with the 'magnitude' being calculated as the square root of the calculated power value. Both magnitude and power are quantities derived from the rate of change of optical path length or velocity and take the units of ms^{-1}.

Alternative measurement techniques (hydrophones) were not used during this work, because the LDV had previously been characterised and compared directly with the UK underwater pressure standard (NPL laser interferometer) and traceable hydrophones at the NPL [25], thus identifying the measurement noise floor, resolution and traceability of the technique. Hence the direct quantified output of the LDV and subsequent computational processing is presented.

3.1. 3 mm diameter object

Previous work [24–28] had already established the ability of the LDV transducer to reliably record and observe acoustic fields within water. The purpose of this research was to consider the consequences of objects being placed within the water-based acoustic field. The format for the experimentation presented here considered three cylindrical bars of various diameters: 3 mm steel bar, 15 mm steel bar and 12 mm aluminium alloy tube. Clearly these are predominantly two-dimensional objects with a very large aspect ratio. By aligning these objects parallel to the laser beam, perpendicular to the acoustic axis, the predominant acoustic scattering

was found to be in the direction perpendicular to the laser beam, thus maximising the measured effect. Furthermore, while these objects were not defined as being infinite, their length dimension exceeded the width of the acoustic field meaning that the acoustic energy was only incident on the curved surfaces of each object.

A collimated planar acoustic tone burst was produced using a Met-Optic Plane piston source transducer operating at 180 kHz with a tone-burst duration of 5 or 10 complete cycles. The transducer to object distance was 100 mm, and with an average water temperature of 16.5 °C, the acoustic wavelength was calculated to be 8.17 mm using Coppens mathematical approximation [4]. The diameter of the acoustic transmission was approximately 50 mm, transmitting along the length of the tank. A time history of the rate of change of optical path length was recorded at 4134 target grid positions, with the duration of the time history specified as 102.4 μs. with a resolution of 0.1 μs. This experimental detail is summarised in Table 1 for all three obstructions used during the work.

Three quantified time-sliced images are presented in Fig. 4, depicting the passage of the acoustic tone burst through water in which the 3 mm bar is suspended, at three discrete time instants. Fig. 4(c) shows a number of concentric acoustic pressure waves emanating from the bar. It is probable that this scattering of acoustic energy occurs throughout the duration of the tone burst, but due to the low amplitude of the scattered waves by comparison with the principal tone burst, their presence cannot be identified in the time-resolved images until the principal tone burst has passed. It is worthy of note that the ratio of the dimension of this obstacle to the acoustic wavelength ($3/8.17 = 0.37$) is significantly less than the widely accepted threshold at which the scattering is assumed to be significant, where the obstacle is of the same order as the acoustic wavelength.

Analysis of the FFT and DFT components of the data reveal that the acoustic power distribution is high in the region to the left of the 3 mm diameter obstacle and in a number of 'streams' passing either side of the bar at increasingly diverging angles. Another important feature of the images in Fig. 4 is the interference patterns evident throughout the field. These are particularly apparent in areas of low acoustic 'power' such as the region immediately beyond the bar. Here a diagonal pattern of interference can be clearly observed.

In addition to the reflected component of the acoustic wave, consideration has been given to the component transmitted into the bar at the water/steel boundary. A proportion of this transmitted wave is reflected at the steel/water boundary at the far side of the bar, while the remainder is transmitted back into the water. Given that the speed of sound in steel, ($c_{\text{steel}} = 5050$ m/s [38]) is much greater than that in water ($c = 1471.1$ m/s at 16.5 °C), any acoustic energy which has passed through the bar and returned to the water would be expected to propagate in advance of the remainder of the acoustic energy. The distance by which this component leads, d_{lead}, the remainder can be calculated by determining the time taken, t_{bar}, for the acoustic wave to travel through the steel bar with diameter, d_{bar},

$$d_{\text{lead}} = d_{\text{bar}} - ct_{\text{bar}} = d_{\text{bar}}\left(1 - \frac{c}{c_{\text{steel}}}\right). \tag{5}$$

For the 3 mm diameter steel bar, d_{lead}, is calculated to be 2.13 mm, which corresponds to a phase difference of 0.51π for a 180 kHz acoustic wave in water. This distance is clearly very small with respect to the dimensions of the scanning region, and as such, it is not possible to identify this lead in the magnitude or phase data related to Fig. 4, or subsequent images.

Table 1
Acoustic obstruction detail and parameters

Bar type	Material	Diameter (mm)	Material acoustic velocity (ms^{-1})	Water acoustic wavelength @ 180 kHz (mm)	Target grid positions	Image 1 time (μs)	Image 2 time (μs)	Image 3 time (μs)
Solid	Steel	3.00	5050	8.17	4134	7.5	20.0	30.0
Solid	Steel	15.00	5050	8.17	3600	13.0	20.8	30.0
Hollow	Aluminium	12.00	6300	8.17	4242	13.0	20.8	30.0

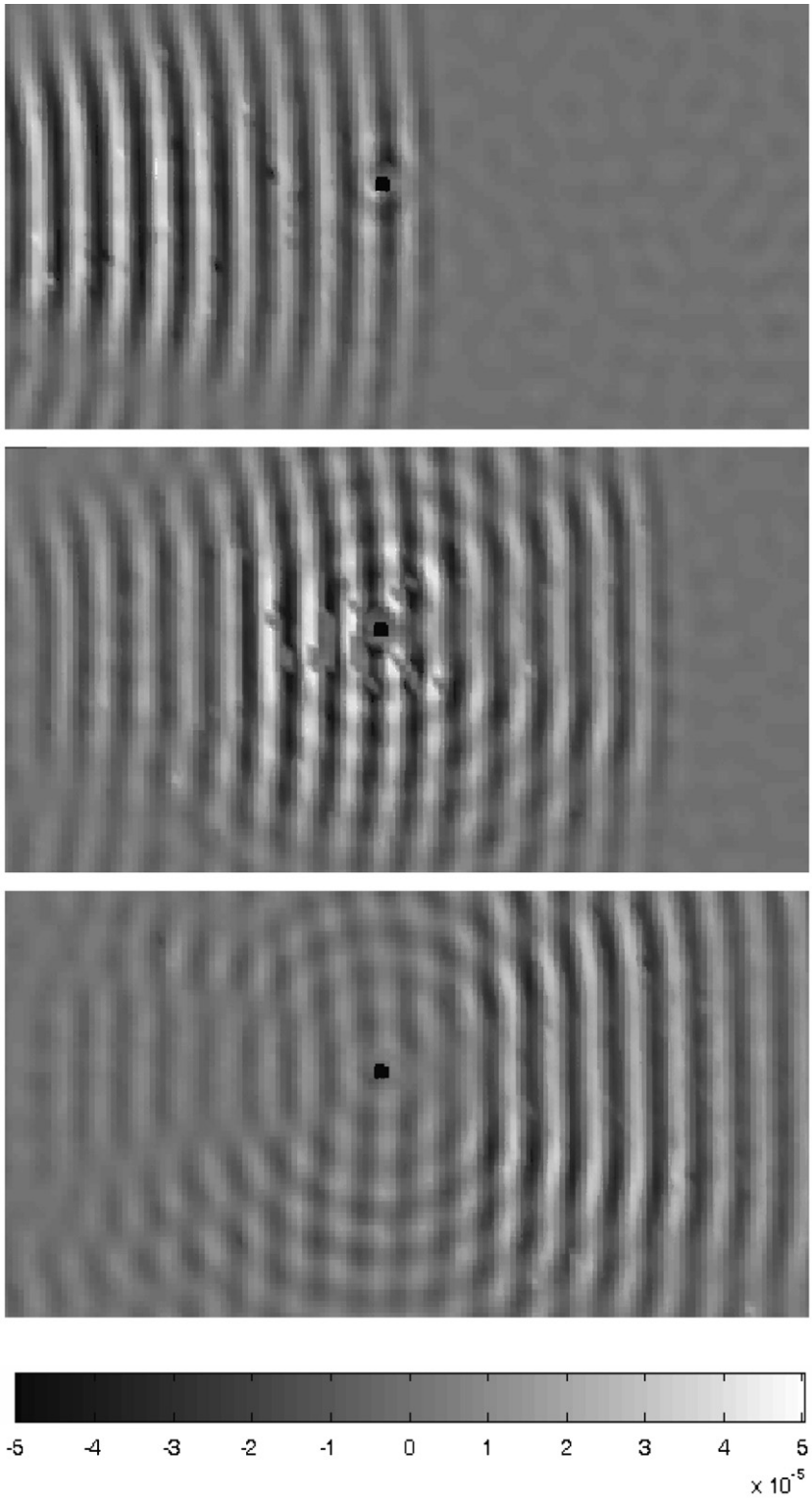

Fig. 4. 180 kHz plane wave tone-burst incident on a 3 mm diameter cylindrical steel bar at three time instants, measured as a rate of change of optical path length (ms^{-1}): (a) $t = 7.5\,\mu s$, (b) $t = 20.0\,\mu s$ and (c) $t = 30.0\,\mu s$.

3.2. 15 mm diameter object

The same procedure was followed in recording measurements of the acoustic scattering caused by the presence of a 15 mm bar within the field. This bar represented an obstruction with dimension greater than the acoustic wavelength with detail summarised in Table 1.

Images representing the rate of change of optical path length at three instants in time are provided in Fig. 5. The presence of scattered acoustic components can be observed in each of the images, with Fig. 5(a) showing interference in the region immediately prior to the obstruction when only 2 cycles have passed the front edge of the bar. This interference becomes more evident in Fig. 5(b) where a complex interference pattern can be observed. Regions of increased and decreased amplitude can be seen with recurring periodicity.

Fig. 5(c) depicts a similar pattern to that observed for each of the previous cylindrical obstructions, where two series of pressure waves can be observed, one representing the principal tone burst and the other the signal scattered by the bar. Further analysis of the FFT data identified significant reduction in power measured in the region immediately to the right of the obstruction, where the power is generally 2 orders of magnitude less than that in the region prior to the bar.

Consideration was also given to the component of the acoustic tone burst transmitted through the 15 mm steel bar. Calculations to establish the position distance of the transmitted wave suggest that it would lead that remainder of the acoustic tone burst by 10.63 mm. This corresponds to a phase lead of 2.6π for a 180 kHz acoustic wave in water. Again a discrepancy in the phase continuity was also observed in the region to the right of the bar in the FFT and DFT data. However, the observed discrepancy is not equal to that calculated from the theory of the transmitted wave. It is unclear at this point in time if the phase discontinuity is a function of the acoustical physics, or a function of the interferometer integration of the complex acoustic wavefronts.

3.3. 12 mm diameter hollow object

In addition to the interrogation of acoustic fields impeded by solid cylindrical objects, attention was given to scattering by a hollow aluminium cylindrical scatterer. Three images are presented in Fig. 6, depicting the tone burst at three time instants, summarised in detail in Table 1.

The principal acoustic tone burst used was identical in frequency and amplitude to those generated in the interrogation of solid bar experiments. It is significant therefore, that the amplitude scale used for the time-resolved images depicted in Figs. 4 and 5 was required to be increased by 50% from that used for the equivalent images from the solid bar experiments. This was necessary to cater for the magnitude of the regions of constructive interference between the principal tone burst and scattered acoustic energy. This suggests that the strength of the signal scattered from the 12 mm aluminium tube was greater than that of the signal scattered by the 15 mm solid steel bar.

It is known that an acoustic wave incident on a boundary between one medium and another will generate a reflected and a transmitted wave [38]. There are two such boundaries in this case: the water/aluminium of the outer diameter of the tube and the aluminium/water of the inner diameter. However, the resolution and detail of the existing experimentation is not sufficient to determine any specific contributions.

This research also offered the opportunity to study the acoustic propagation through the water within the centre of the tube, in a similar manner to that seen in air [17]. In each of the images depicted, continuity between positions of equal phase is observed to extend through this region, suggesting that a proportion of the acoustic energy is transmitted through the aluminium hollow tube and into the water behind.

An examination of the phase in the region to the right of the bar again showed inconsistencies. However, in this case it might be argued that the influence of the acoustic wave transmitted through the aluminium is greater than was the case with the steel bars through close scrutiny of the time-resolved image shown in Fig. 6(a). Here, a feint region depicting the first positive rate of change of optical path length of a propagating tone burst can be identified at a position ahead of the remainder of the field. However, the resolution of the data is limited, and higher resolution experiments are required before firm conclusions can be drawn on this matter.

Comprehensive theoretical studies of the relative strengths of reflected and transmitted acoustic signals from different material solid surfaces have previously been produced [38–40]. While the exact experimental scenario

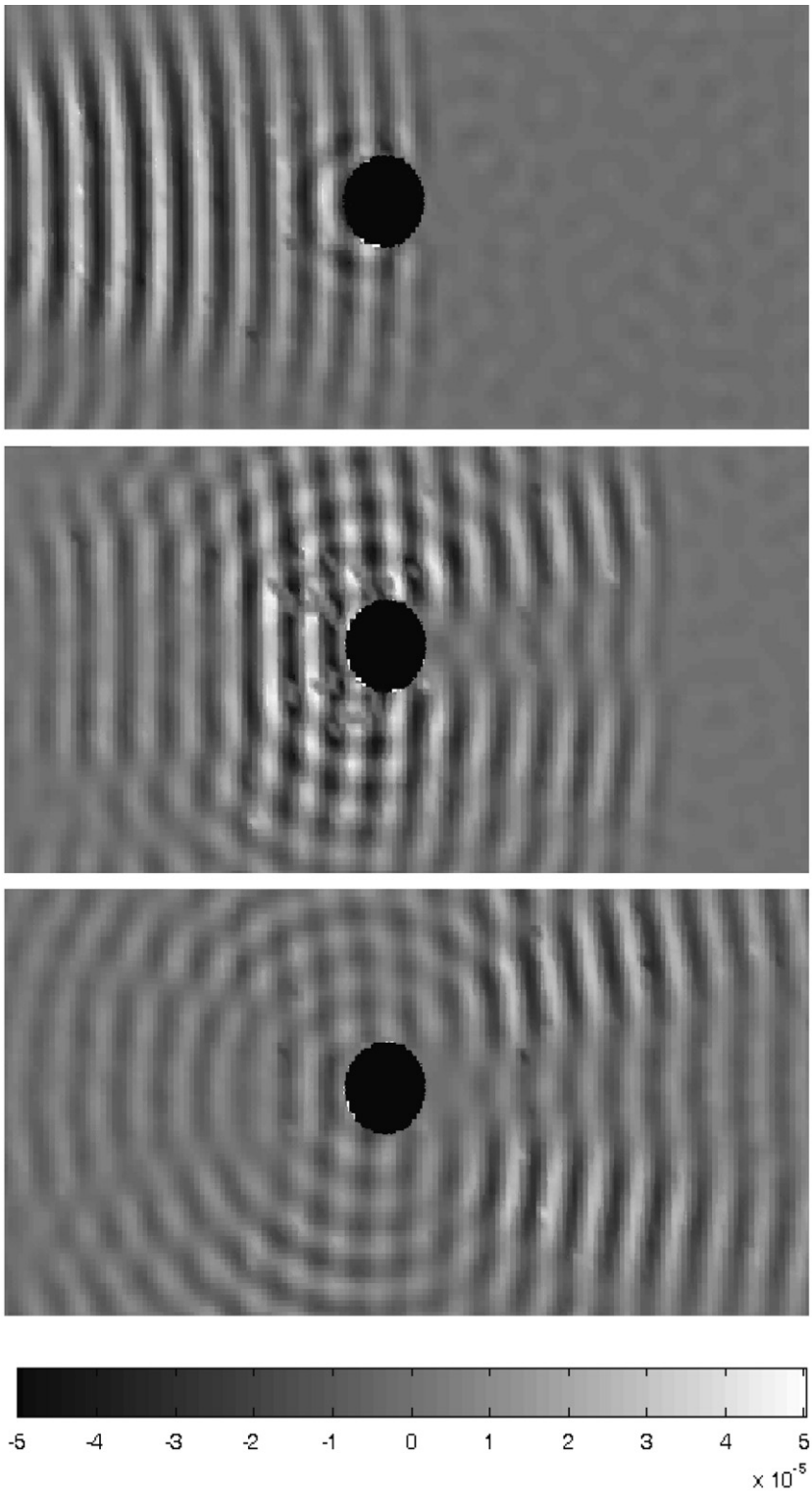

Fig. 5. 180 kHz plane wave tone-burst incident on a 15 mm diameter cylindrical steel bar at three time instants, measured as a rate of change of optical path length (ms^{-1}): (a) $t = 7.5\,\mu s$, (b) $t = 20.0\,\mu s$ and (c) $t = 30.0\,\mu s$.

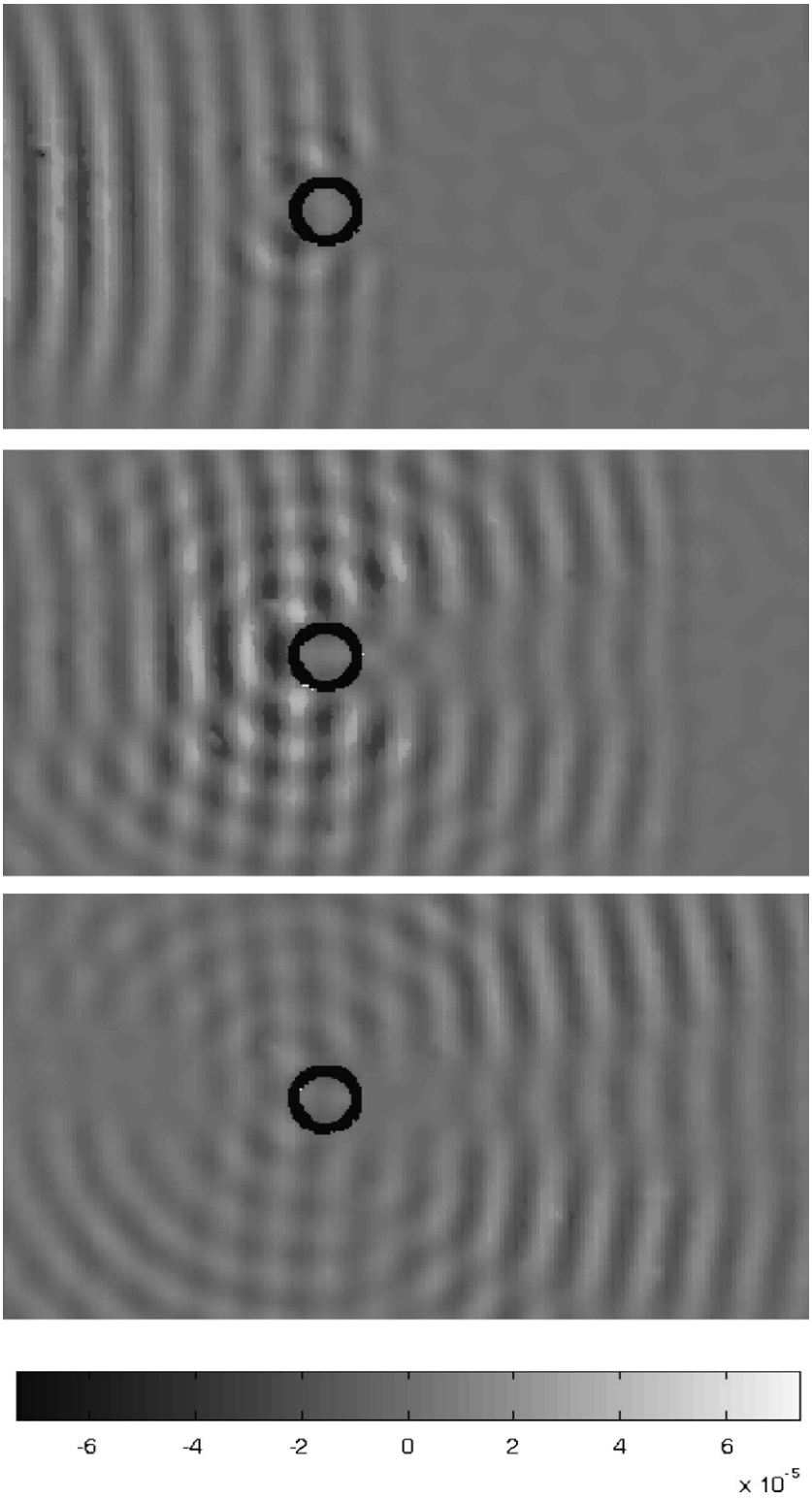

Fig. 6. 180 kHz plane wave tone-burst incident on a 12 mm diameter cylindrical aluminium alloy tube at three time instants, measured as a rate of change of optical path length (ms^{-1}): (a) $t = 7.5\,\mu s$, (b) $t = 20.0\,\mu s$ and (c) $t = 30.0\,\mu s$.

described here is not discussed in these works, consideration is given to the reflection and transmission of acoustic waves normally incident on solid and cylindrical surfaces. In all three cases, these reports (and others) provide a potential basis of understanding and correlating the data generated from the Laser Doppler vibrometer.

The significant difference is that these texts report experiments detailing pressure measurements, while the data reported here is presented as rate of change of path length (refractive index). Hence, a quantitative correlation would be inappropriate (and is not possible at this stage), especially due to the issues of complex integration of pressure terms through the acoustic volume. Consequently, this current work has been completed to demonstrate the potential applicability of the laser Doppler vibrometer to wholefield water-based acoustical analysis, but not as a direct comparison to acoustical theory.

In order to progress to quantitative comparison and correlation with theoretical models, the following elements of the instrumentation and experimentation need to be addressed in the future; increased resolution of measurement through smaller scan steps, better understanding of the integration of complex pressure terms along the line of laser interrogation, and consequently the derivation of a global error map for the experiment as a function of scan angle.

4. Conclusions

The experimentation reported here has demonstrated the unique potential of laser Doppler vibrometry as a non-perturbing optical method for visualising acoustic scattering from objects within a volume. The influence of the localised changes in pressure cause corresponding changes in the refractive index of the water, which are detected as path length changes by the scanning Laser Doppler vibrometer.

Measurements made using the vibrometer take the units of metres per second, by virtue of the fact that it provides a measurement of the rate of change of optical path length. While it is not currently possible to present the resultant quantified images depicting the spatial and temporal distributions of acoustic parameters in conventional acoustic units, the features exhibited in the data (reflection and refraction) are representative of the acoustic scattering caused by the obstacle.

These initial results provide a rapid and unique ability to increase understanding of water-based acoustic scattering, although further detailed experimentation is necessary to improve signal resolution, confirm data integrity, derive transform functions and generate wholefield error mapping, before correlation to appropriate acoustics theory can be achieved. However, the potential for this technique to be applied to many liquid acoustic-based applications is self-evident, and provides potential to better understand the engineering and acoustic consequences of structures within acoustic fields.

Acknowledgements

The authors gratefully acknowledge the support of Roy Preston and Stephen Robinson from the National Physical Laboratory, UK, for their assistance with the experimentation reported in this work and to Roger Traynor of Lambda Photometrics for the loan of the Polytec scanning LDV and similar equipment.

References

[1] V.A. Del Grosso, New equations for the speed of sound in natural waters (with comparison to other equations), *Journal of the Acoustical Society of America* 56 (4) (1974) 1084–1091.

[2] C.T. Chen, F.J. Millero, Speed of sound in seawater at high pressures, *Journal of the Acoustical Society of America* 62 (5) (1977) 1129–1135.

[3] K.V. Mackenzie, Nine term equation for the speed of sound in the oceans, *Journal of the Acoustical Society of America* 70 (3) (1981) 807–812.

[4] A.B. Coppens, Simple equations for the speed of sound in Neptunian waters, *Journal of the Acoustical Society of America* 69 (3) (1981) 862–863.

[5] R.C. Preston, The NPL ultrasound beam calibrator, *IEEE Transactions on Ultrasonics, Ferroelectrics and Frequency Control* 35 (2) (1988) 122–139.

[6] L.E. Drain, J.H. Speake, B.C. Moss, Displacement and vibration measurement by laser interferometry, *Proceedings of the European Congress on Optics applied to Metrology, SPIE* 136 (1977) 52–57.
[7] D.R. Bacon, L.E. Drain, B.C. Moss, R.A. Smith, A new primary standard for hydrophone calibrations, *Physics in Medical Ultrasound, Institute of Physical Sciences in Medicine* 47 (1986) 30–35.
[8] D.R. Bacon, Primary calibration of ultrasonic hydrophones using optical interferometry, *IEEE Transactions on Ultrasonics, Ferroelectrics and Frequency Control* 35 (2) (1988) 152–161.
[9] R. Debeye, F. Sears, On the scattering of light by supersonic waves, *Proceedings of the National Academy of Sciences* 18 (1932) 409.
[10] R. Lucas, P. Biquard, Properties optiques des milieux solides et liquids soumis aux vibrations elastiques ultra sonores, *Journal of Physique Radium—7th Series* 3 (1932) 464–477.
[11] C.V. Raman, N.S.N. Nath, The diffraction of light by high frequency sound waves: Part I, *Proceedings of the Indian Academy of Science* 2 (1935) 406–412.
[12] C.V. Raman, N.S.N. Nath, The diffraction of light by high frequency sound waves: Part II, *Proceedings of the Indian Academy of Science* 2 (1935) 413–420.
[13] B.D. Cook, The measurement of high frequency sound fields using optical techniques, *SPIE* 2358 (1994) 278–280.
[14] H.G. Jerrard, Birefringence induced in liquids and solutions by ultrasonic waves, *Ultrasonics* (1954) 74–81.
[15] D.R. Bacon, Primary calibration of ultrasonic hydrophones using optical interferometry, *IEEE Transactions on Ultrasonics, Ferroelectrics and Frequency Control* 35 (2) (1988) 152–161.
[16] R. Rustad, O.J. Lokberg, H.M. Pedersen, K. Klepsvik, T. Storen, TV holography measurements of underwater acoustic fields, *Journal of the Acoustical Society of America* 102 (3) (1997) 1904–1906.
[17] N.-E. Molin, L. Zipser, Optical methods of today for visualizing sound fields in musical acoustics, *Acta Acustica* 90 (2004) 618–628.
[18] K.J. Taylor, Absolute measurement of acoustic particle velocity, *Journal of the Acoustical Society of America* 59 (3) (1976) 691–694.
[19] L. Zipser, H. Franke, E. Olsson, N.-E. Molin, M. Sjödahl, Reconstructing two-dimensional acoustic object fields by use of digital phase conjugation of scanning laser vibrometry recordings, *Applied Optics* 42 (29) (2003) 5831–5838.
[20] L. Zipser, H. Franke, Laser-scanning vibrometry for ultrasonic transducer development, *Sensors and Actuators A* 110 (2004) 264–268.
[21] S. Vanlanduit, J. Vanherzeele, P. Guillaume, G. De Sitter, Absorption measurement of acoustic materials using a scanning laser Doppler vibrometer, *Journal of the Acoustical Society of America* 117 (3) (2005) 1168–1172.
[22] J. Huang, J.D. Achenbach, Dual-probe laser interferometer, *Journal of the Acoustical Society of America* 90 (3) (1991) 1269–1274.
[23] Y. Wang, Y. Huang, Calibration of hydrophones using optical technique, *Acta Acustica (China)* 26 (1) (2001) 29–33.
[24] A.R. Harland, J.N. Petzing, J.R. Tyrer, Non-invasive measurements of underwater pressure fields using laser Doppler velocimetry, *Journal of Sound and vibration* 252 (1) (2002) 169–171.
[25] A.R. Harland, J.N. Petzing, J.R. Tyrer, C.J. Bickley, S.P. Robinson, R.C. Preston, Application and assessment of laser Doppler velocimetry for underwater acoustic measurements, *Journal of Sound and Vibration* 265 (3) (2003) 627–645.
[26] G.P. Carroll, Measurements of underwater acoustic pressure fields using scanning laser Doppler vibrometry, *Proceedings of the 147th Meeting of the Acoustical Society of America*, 4pSA2, New York, May 2004.
[27] A.R. Harland, J.N. Petzing, J.R. Tyrer, Non-perturbing measurements of spatially distributed underwater acoustic fields using a scanning laser Doppler vibrometer, *Journal of the Acoustical Society of America* 115 (1) (2004) 187–195.
[28] A.R. Harland, The Application of Laser Doppler Velocimetry to the Measurement of Underwater Acoustic Fields, PhD Thesis, Loughborough University, UK, 2002.
[29] J.M. Buick, J.A. Cosgrove, P.-A. Douissard, C.A. Greated, B. Gilabert, Application of the acousto-optic effect to pressure measurements in ultrasound fields in water using a laser vibrometer, *Review of Scientific Instruments* 75 (10) (2004) 3203–3207.
[30] G. Madelin, B. Hosten, C. Biateau, C. Mougenot, J.-M. Franconi, E. Thiaudière, Comparison of laser interferometry and radiation force method of measuring ultrasonic power, *Ultrasonics* 43 (2005) 769–774.
[31] P.D. Theobald, S.P. Robinson, A.D. Thompson, R.C. Preston, P.A. Lepper, W. Yuebing, Technique for the calibration of hydrophones in the frequency range 10 to 600 kHz using a heterodyne interferometer and an acoustically compliant membrane, *Journal of the Acoustical Society of America* 118 (5) (2005) 3110–3116.
[32] R. Mattsson, Bending and acoustic waves in a water-filled box studied by pulsed TV holography and LDV, *Optics and Lasers in Engineering* 44 (2006) 1146–1157.
[33] D.C. Williams, *Optical Methods in Engineering Metrology*, Chapman & Hall, London, 1993.
[34] C.J.D. Pickering, N.A. Halliwell, The laser vibrometer: a portable instrument, *Journal of Sound and Vibration* 107 (3) (1986) 471–485.
[35] BS ISO 16063-1:1998, Methods for the calibration of vibration and shock transducers—Part 1: basic concepts.
[36] Polytec GmbH, *Manufacturer calibration procedure for laser vibrometers*, Issue 07, 2002, Polytec GmbH, Polytec-Platz 1-7, D76337, Waldbronn, Germany.
[37] The MathWorks, *Signal Processing Toolbox, Users Guide Version 5*, The MathWorks Inc., Natick, MA, USA, 2000.
[38] L.E. Kinsler, A.R. Frey, A.B. Coppens, J.V. Sanders, *Fundamentals of Acoustics*, fourth ed., Wiley, New York, 2000.
[39] J.R. Faran, Sound scattering by solid cylinders and spheres, *Journal of the Acoustical Society of America* 23 (4) (1951) 405–418.
[40] Y.E. Zhen, Recent developments in underwater acoustics: acoustic scattering from single and multiple bodies, *Proceedings of the National Science Council ROC(A)* 25 (3) (2001) 137–150.